

PURDUE UNIVERSITY
GRADUATE SCHOOL
Thesis/Dissertation Acceptance

This is to certify that the thesis/dissertation prepared

By Qiaoqiao Wan

Entitled

Effects of Shear Stress on RhoA Activities and Cytoskeletal Organization in Chondrocytes

For the degree of Master of Science in Biomedical Engineering

Is approved by the final examining committee:

Sungsoo Na

Chair

Hiroki Yokota

Jiliang Li

To the best of my knowledge and as understood by the student in the *Research Integrity and Copyright Disclaimer (Graduate School Form 20)*, this thesis/dissertation adheres to the provisions of Purdue University's "Policy on Integrity in Research" and the use of copyrighted material.

Approved by Major Professor(s): Sungsoo Na

Approved by: John H. Schild

Head of the Graduate Program

05/07/2012

Date

**PURDUE UNIVERSITY
GRADUATE SCHOOL**

Research Integrity and Copyright Disclaimer

Title of Thesis/Dissertation:

Effects of Shear Stress on RhoA Activities and Cytoskeletal Organization in Chondrocytes

For the degree of Master of Science in Biomedical Engineering

I certify that in the preparation of this thesis, I have observed the provisions of *Purdue University Executive Memorandum No. C-22*, September 6, 1991, *Policy on Integrity in Research*.*

Further, I certify that this work is free of plagiarism and all materials appearing in this thesis/dissertation have been properly quoted and attributed.

I certify that all copyrighted material incorporated into this thesis/dissertation is in compliance with the United States' copyright law and that I have received written permission from the copyright owners for my use of their work, which is beyond the scope of the law. I agree to indemnify and save harmless Purdue University from any and all claims that may be asserted or that may arise from any copyright violation.

Qiaoqiao Wan

Printed Name and Signature of Candidate

05/16/2012

Date (month/day/year)

*Located at http://www.purdue.edu/policies/pages/teach_res_outreach/c_22.html

EFFECTS OF SHEAR STRESS ON RHOA ACTIVITIES
AND CYTOSKELETAL ORGANIZATION IN CHONDROCYTES

A Thesis

Submitted to the Faculty

of

Purdue University

by

Qiaoqiao Wan

In Partial Fulfillment of the

Requirements for the Degree

of

Master of Science in Biomedical Engineering

August 2012

Purdue University

Indianapolis, Indiana

ACKNOWLEDGMENTS

This study and graduate thesis could not be completed without the kind attention and careful guidance from my advisor Dr. Sungsoo Na. His serious scientific attitude, his spirit of rigorous scholarship and his work style of always pursuing improvement deeply influenced and inspired me. From the beginning of the topic selection to the final completion of the thesis, Dr. Sungsoo Na was consistently giving me guidance and support. Over these two years, Dr. Na not only guided me on academic field, but also took care and be concerned about my life. As an international student studied here alone, I would like to extend my sincere thanks to him.

Here, I thank my co-adviser Dr. Hiroki Yokota, without his support and his academic assistance, I can not finish this research. I really appreciate my committee member Dr. Jiliang Li. It is precisely because of their help and support; I can overcome the difficulties one by one until the successful completion of the paper. And I thank Dr. Matsuda, Dr. Tsien, Dr. Wang for providing important reagents for this study.

Many honorable teachers, classmates, friends and department staff gave me speechless help, here please accept my sincere thanks!

Finally, I really want to say “thank you” to my parents who raised me up and educated me to be a decent person.

TABLE OF CONTENTS

	Page
LIST OF FIGURES	iv
ABSTRACT	vii
1 INTRODUCTION	1
2 MATERIALS AND METHODS	4
2.1 DNA Plasmids	4
2.2 Cell Culture and Transfection	4
2.3 Inhibitors	6
2.4 Traction Force Microscopy	6
2.5 Shear Stress Application and Microscopy	6
2.6 Statistical Analysis	8
3 RESULTS	10
3.1 Selective RhoA Activity is Regulated by the Magnitude of Shear Stress	10
3.2 Shear Stress-induced RhoA Activity is Correlated with F-actin Remod- eling	17
3.3 Actin and Intracellular Tension are Necessary for Shear Stress-induced RhoA Activity	17
3.4 Shear Stress Regulates Traction Forces	21
3.5 Intermediate Shear Stress Decreases Constitutively Activated RhoA	21
4 DISCUSSION	27
LIST OF REFERENCES	29

LIST OF FIGURES

Figure	Page
1.1 Articular cartilage and RhoA protein signaling regulators. (a) Articular cartilage lay between two bone plates. (b) Regulators of RhoA protein signaling activate or inhibit Rho activity.	3
2.1 RhoA biosensor. (a) FRET-based RhoA biosensor used in this study to monitor RhoA activity. (b) YFP/CFP ratio value increases with the activation of RhoA.	5
2.2 Polyacrylamide gel used for traction force experiment. (a) Cells were seeded on the polyacrylamide gel embedded with red fluorescent submicrobeads. (b) The change of cell contraction in response to shear stress was determined by monitoring the bead displacement vector(modified from [34]).	7
2.3 Shear stress experiment device.(a) Cells were seeded on glass cover slip coated with hydrogel, and applied shear flow inside parallel plate flow chamber (Modified from [35]). (b) Transfected cell plated on μ -slide cell culture chamber (Ibidi), and subjected to shear flow. Arrow denoted flow direction.	9
3.1 RhoA activity is shear stress-magnitude dependent. RhoA activity was not altered when shear stress of 2 dyn/cm ² was applied. Shear stress was applied for 1 h. (a) Time course of RhoA activity in response to shear stress. Color bars represent emission ratio of YFP/CFP of the biosensor, an index of RhoA activation. (b) Ratio images of YFP/CFP emission ratio were averaged over the whole cell and were normalized to time point 0 min. Blue color indicates pre- and post-shear stress (no flow), and red color indicates shear stress (2 dyn/cm ²) application. n = 6 cells. Scale bars, 10 μ m. Error bars denote s.e.m.	11
3.2 RhoA activity is shear stress-magnitude dependent. (a,b) In response to shear stress at 5 dyn/cm ² , RhoA activity is inhibited rapidly. (b) n = 5 cells. Scale bars, 10 μ m. Error bars denote s.e.m. The white boxes in 3.2a are cropped and enlarged in 3.2c, for a better visualization.	12
3.3 RhoA activity is shear stress-magnitude dependent. (a,b) the application of 10 dyn/cm ² shear stress led to slow, but strong RhoA activation. (b) n = 7 cells. Scale bars, 10 μ m. Error bars denote s.e.m.	13

Figure	Page
3.4 RhoA activity is shear stress-magnitude dependent. (a,b) 20 dyn/cm ² led to slow, but strong RhoA activation. (b) n = 6 cells. Scale bars, 10 μm. Error bars denote s.e.m. The white boxes in 3.4a are cropped and enlarged in 3.4c, for a better visualization.	14
3.5 Shear stress-induced actin cytoskeleton organization is essential for selective RhoA activation. (a) In response to 5 dyn/cm ² , the cell display a decrease in actin (see arrowheads). Three other different cells showed similar results. (b) The white boxes in 3.5a are cropped and enlarged in 3.5b, for a better visualization. White arrows denote shear flow direction. Scale bars, 10 μm.	15
3.6 Shear stress-induced actin cytoskeleton organization is essential for selective RhoA activation. (a) In response to 20 dyn/cm ² , the actin structure increase (see arrowheads). Three other different cells showed similar results. (b) The white boxes in 3.6a are cropped and enlarged in 3.6b, for a better visualization. White arrows denote shear flow direction. Scale bars, 10 μm.	16
3.7 Shear stress-induced changes in RhoA activity are dependent on actin cytoskeleton and prestress. The cells were transfected with RhoA biosensor and then treated with CytoD (1 μg/ml for 15 min), LatA (1 μM for 15 min) to disrupt F-actin, ML-7 (25 μM for 30 min) to inhibit myosin light chain kinase, or Bleb (50 μM for 20 min) to inhibit myosin II. (a,b) YFP/CFP ratio images show C28/I2 cells pre-incubated with Cyto D, LatA, ML7, or Bleb prevents RhoA inhibition and activation in response to 5 dyn/cm ² and 20dyn/cm ² , respectively. (c) n= 3 cells for CytoD, n = 4 cells for LatA, n = 4 cells for ML-7, n = 2 cells for Bleb.(d) n= 4 cells for CytoD, n = 3 cells for LatA, n = 4 cells for ML-7, n = 3 cells for Bleb. Scale bars, 10 μm. Error bars denote s.e.m.	18
3.8 Dynamic tractions are regulated by stress-magnitude dependent. Dynamic traction maps and time courses of averaged tractions in response to 5 dyn/cm ² . (a) Color bars represent traction values in pascal (Pa). White arrows indicate shear stress direction. Insets are corresponding DIC images. (b) n = 5 cells. Value are normalized by the tractions at 0 min. For the statistical analysis, traction at 20 min and 60 min were compared with traction at 0 min (* P < 0.05). Scale bars, 10 μm. Error bars denote s.e.m.	22

Figure	Page
3.9 Dynamic tractions are regulated by stress-magnitude dependent. Dynamic traction maps and time courses of averaged tractions in response to 20 dyn/cm ² . (a) Color bars represent traction values in pascal (Pa). White arrows indicate shear stress direction. Insets are corresponding DIC images. (b) n = 5 cells. Value are normalized by the tractions at 0 min. For the statistical analysis, traction at 60 min were compared with traction at 0 min (* P < 0.05). Scale bars, 10 μm. Error bars denote s.e.m.	23
3.10 Shear stress of 5 dyn/cm ² downregulate RhoA activity of the cell transfected with a constitutively active RhoA, however, 20 dyn/cm ² fail to activate RhoA activity further. (a) RhoA activity decreases in response to 5 dyn/cm ² and 20 dyn/cm ² . White arrows denote shear stress direction. (b) n = 3 cells for 5 dyn/cm ² and 20 dyn/cm ² . Scale bars, 10 μm. Error bars denote s.e.m.	24
3.11 RhoA-N19 blocked the RhoA regulation by shear stress. (a) The dominant negative N19 RhoA transfection prevents shear stress-induced RhoA activity in both stress conditions. (b) n=4 cells for both 5 dyn/cm ² and 20 dyn/cm ² . Scale bars, 10 μm. Error bars denote s.e.m.	25
3.12 C3 transferase blocked the RhoA regulation by shear stress. (a) Preincubation of C3 transferase prevents shear-stress-induced RhoA activity in both stress conditions. (b) n=3 cells for 5 dyn/cm ² and 4 for 20 dyn/cm ² . Scale bars, 10 μm. Error bars denote s.e.m.	26

ABSTRACT

Wan, Qiaoqiao. M.S.B.M.E., Purdue University, August 2012. Effects of Shear Stress on RhoA Activities and Cytoskeletal Organization in Chondrocytes. Major Professor: Sungsoo Na.

Mechanical force environment is a major factor that influences cellular homeostasis and remodeling. The prevailing wisdom in this field demonstrated that a threshold of mechanical forces or deformation was required to affect cell signaling. However, by using a fluorescence resonance energy transfer (FRET)-based approach, we found that C28/I2 chondrocytes exhibited an increase in RhoA activities in response to high shear stress (10 or 20 dyn/cm²), while they showed a decrease in their RhoA activities to intermediate shear stress at 5 dyn/cm². No changes were observed under low shear stress (2 dyn/cm²). The observed two-level switch of RhoA activities was closely linked to the shear stress-induced alterations in actin cytoskeleton and traction forces. In the presence of constitutively active RhoA (RhoA-V14), intermediate shear stress suppressed RhoA activities, while high shear stress failed to activate them. Collectively, these results herein suggest that intensities of shear stress are critical in differential activation and inhibition of RhoA activities in chondrocytes.

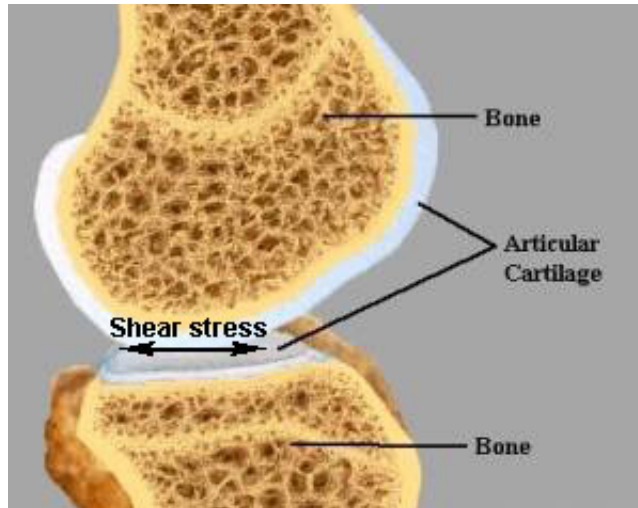
1. INTRODUCTION

Mechanical forces within a physiological range are an important regulator for insuring tissue homeostasis and remodeling [1] [2] [3] [4]. In vivo studies show that flow-induced shear in articular cartilage (Figure 1.1a) stimulates a repair response [5] [6]. Deviations from this physiological loading condition, in contrast, often result in pathological outcomes associated with various diseases [7] [8]. Moderate mechanical loading, for instance, is reported to decrease proteolytic activities of degenerative enzymes in the articular cartilage, while excessive loading may lead to an increase in expression of matrix metalloproteinases [9]. Although substantial progress has been made toward the understanding of how cells sense mechanical forces and convert them into biochemical signals [10] [11] [12] [13] [14], it is not well understood how cells perceive and differentially respond to a wide spectrum of mechanical forces depending on their intensities.

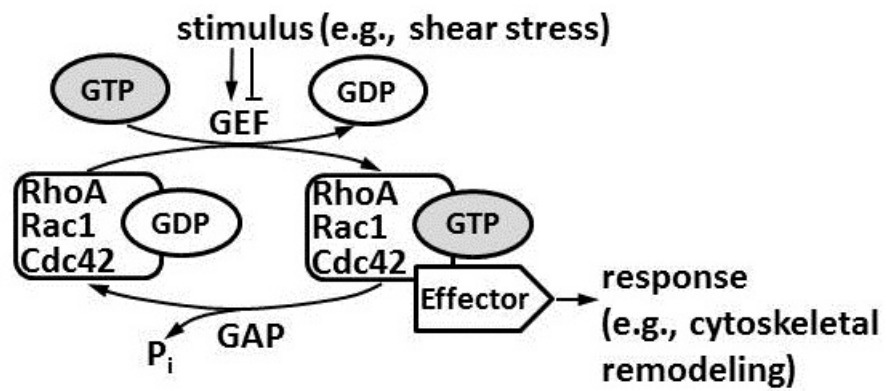
In this study, we investigated the role of RhoA in response to fluid flow-induced shear stress in individual chondrocytes. Recent reports have demonstrated that mechanical forces regulate RhoA activation in many types of cells including endothelial cells [15] [16] [17], smooth muscle cells [18] [19], cardiomyocytes [20], and chondrocytes [21] [22]. RhoA is a member of the family of Rho GTPases that act as a molecular switch in the early mechanotransduction responses [23] [24]. The activity of Rho GTPases can be changed by several GTPases regulators (Figure 1.1b). RhoA regulates a number of intracellular signaling cascades that elicit changes in gene expression and cellular functions including remodeling of actin cytoskeleton and exertion of traction forces [25] [26]. When activated by mechanical force, RhoA regulates multiple downstream effectors. One of the downstream effectors, Rho-associated kinase (ROCK), promotes the assembly of actin cytoskeleton and phosphorylation of myosin light chains. By regulating intracellular tension through the cytoskeleton, this

RhoA-ROCK signaling alters cell shape, and migration patterns as well as cellular differentiation [27].

The specific question addressed in this study was whether different magnitude of shear stress can dissimilarly regulate RhoA activity in C28/I2 chondrocytes. Based on differential regulation of matrix metalloproteinases in response to moderate and acute loading, we hypothesized that RhoA activity can be both reduced and elevated by shear stress depending on its intensity. In order to monitor shear stress-modulated RhoA activity with high spatiotemporal resolution, we employed a fluorescence resonance energy transfer (FRET)-based approach [28]. This FRET approach allowed us to determine time-course dynamical activities of RhoA in individual live cells under shear stress at 2 - 20 dyn/cm² before, during, and after fluid flow treatment. We used a FRET-based RhoA biosensor as well as constitutively active RhoA mutant.



(a)



(b)

Fig. 1.1. Articular cartilage and RhoA protein signaling regulators. (a) Articular cartilage lay between two bone plates. (b) Regulators of RhoA protein signaling activate or inhibit Rho activity.

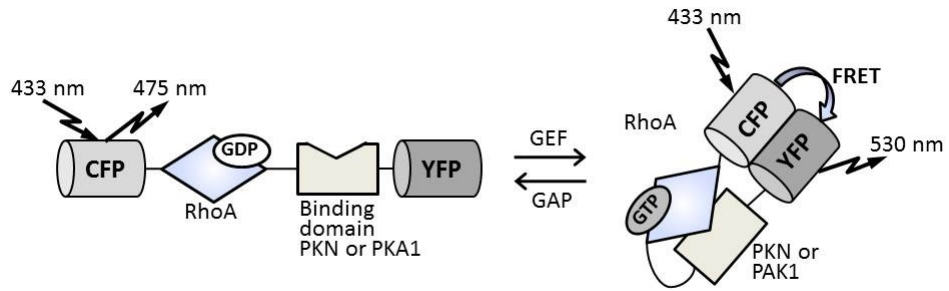
2. MATERIALS AND METHODS

2.1 DNA Plasmids

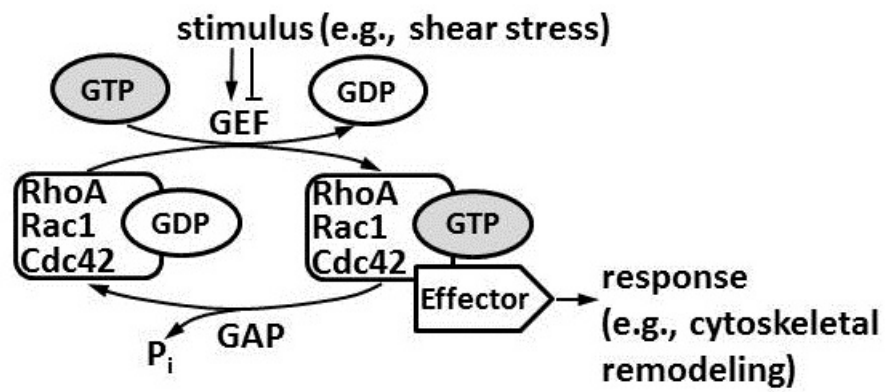
We used a FRET-based, cyan fluorescent protein (CFP)-yellow fluorescent protein (YFP) RhoA biosensor (Raichu-RhoA)(Figure 2.1a), a gift of Dr. M. Matsuda [28]. The probe consists of truncated RhoA, a RhoA binding domain (RBD) of an effector protein, and a pair of CFP&YFP. The intramolecular binding of active RhoA to RBD leads to the close association of CFP with YFP, resulting in an increase of FRET from CFP to YFP. Thus, the FRET activity of the RhoA biosensor was monitored to determine RhoA activity(Figure 2.1b). The RhoA biosensor has been very well characterized in terms of its specificity [28]. As RhoA mutants, a constitutively active RhoA (RhoA-V14) and a dominant negative RhoA (RhoA-N19) were used [29]. An mCherry-actin probe was a gift of Dr. R.Tsien.

2.2 Cell Culture and Transfection

Human chondrocyte cell line, C28/I2, was used for this study [30]. Cells were cultured in Dulbeccos modified Eagles medium (DMEM; Lonza) containing 10% FBS (Hyclone) and 1% penicillin/streptomycin (Lonza) and maintained at 37°C and 5% CO₂ in a humidified incubator. The DNA plasmids were transfected into the cells by using Neon transfection system (Invitrogen) according to the product protocols. After transfection, the cells were transferred to a type I collagen-coated μ -slide cell culture chamber (Ibidi) and incubated in DMEM containing 0.5% FBS for 24-36 h before imaging experiments.



(a)



(b)

Fig. 2.1. RhoA biosensor. (a) FRET-based RhoA biosensor used in this study to monitor RhoA activity. (b) YFP/CFP ratio value increases with the activation of RhoA.

2.3 Inhibitors

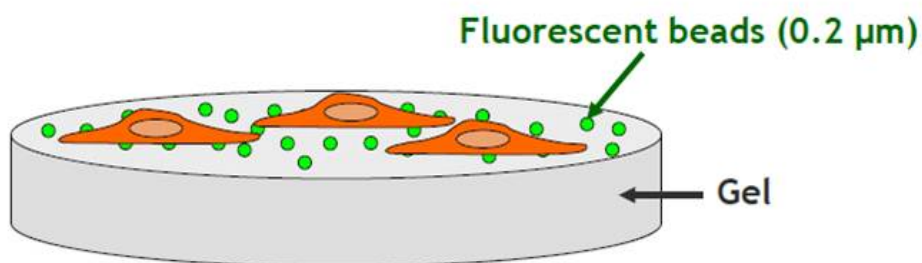
Cytochalasin D and latrunculin A were purchased from Enzo life sciences. Blebbistatin was from Toronto research. ML-7 was from Biomol. C3 transferase was from Cytoskeleton.

2.4 Traction Force Microscopy

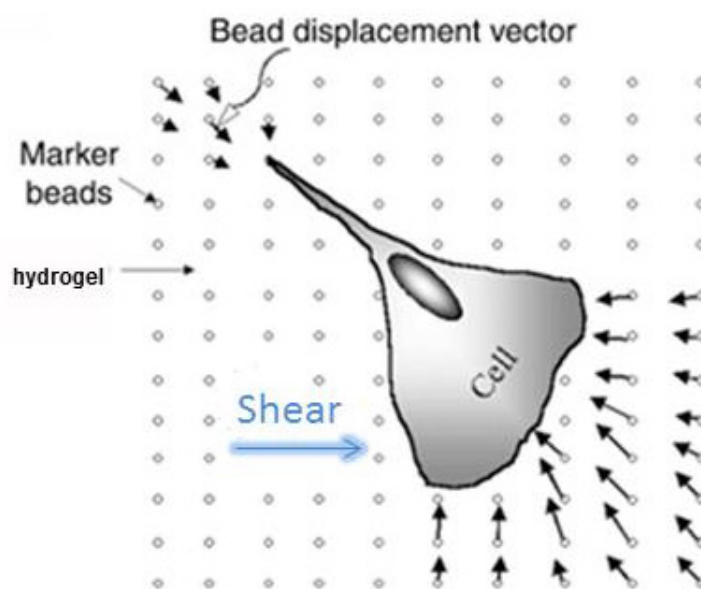
Polyacrylamide gel was used for traction measurements [31]. The elastic Youngs modulus of the gels used in this study was 35 kPa (0.3% bisacrylamide and 10% acrylamide, both purchased from Bio-Rad), which is close to the microscale stiffness of cartilage [32]. Red fluorescent submicrobeads (0.2 μm in diameter; Invitrogen) were embedded in the polyacrylamide gel to track the deformation of the gel(Figure 2.2a). Images of the same region of the gel were taken at different times before or after experimental interventions. The displacement field was determined by monitoring the changes in the position of corresponding fluorescent beads between the reference (cell free) image and the image containing a cell(Figure 2.2b). The traction map was calculated from the displacement field of the fluorescent beads by implementing the solution described previously [33].

2.5 Shear Stress Application and Microscopy

During imaging, a unidirectional flow was applied to the cells grown in the parallel plate flow chamber(Figure 2.3a) or μ -slide cell culture chamber (Ibidi)(Figure 2.3b) without serum at 37°C. Shear stress of 2-20 dyn/cm^2 was applied to the chamber by controlling the flow rate of the peristaltic pump (Cole-Parmer). A pulse dampener (Cole-Parmer) was used to minimize pulsation of the flow. All images were obtained by using an automated fluorescence microscope (Nikon) equipped with an electron-multiplying charge-coupled device (EMCCD) camera (Photometrix), a filter wheel controller (Sutter) and a Perfect Focus System (PFS; Nikon) that maintains the



(a)



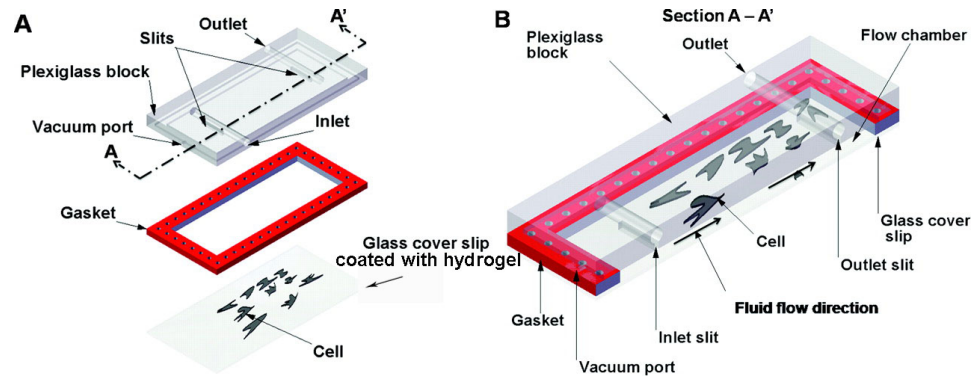
(b)

Fig. 2.2. Polyacrylamide gel used for traction force experiment. (a) Cells were seeded on the polyacrylamide gel embedded with red fluorescent submicrobeads. (b) The change of cell contraction in response to shear stress was determined by monitoring the bead displacement vector(modified from [34]).

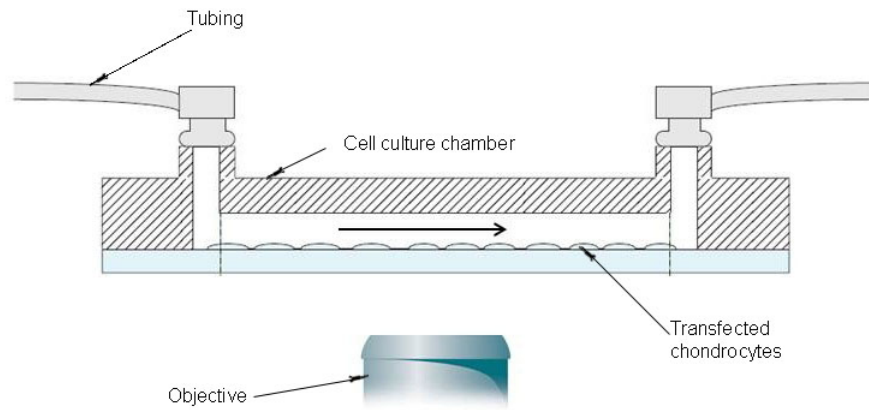
focus during time-lapse imaging. The following filter sets were used (Semrock): CFP excitation: 438/24 (center wavelength/bandwidth in nm); CFP emission (483/32); YFP (FRET) emission: 542/27; mCherry excitation: 562/40; mCherry emission: 641/75. Cells were illuminated with a 100 W Hg lamp through an ND64 ($\sim 1.5\%$ transmittance) neutral density filter to minimize photobleaching. Time-lapse images were acquired at an interval of 2 min with a X63 (0.75 numerical aperture) objective. FRET images for RhoA activity was generated with NIS-Elements software (Nikon) by computing emission ratio of YFP/CFP for the individual cell.

2.6 Statistical Analysis

All statistical data were presented as the mean \pm standard error of the mean (SEM). One-way ANOVA was used to determine the statistical differences during time course experiments. The P-value less than 0.05 was considered significant.



(a)



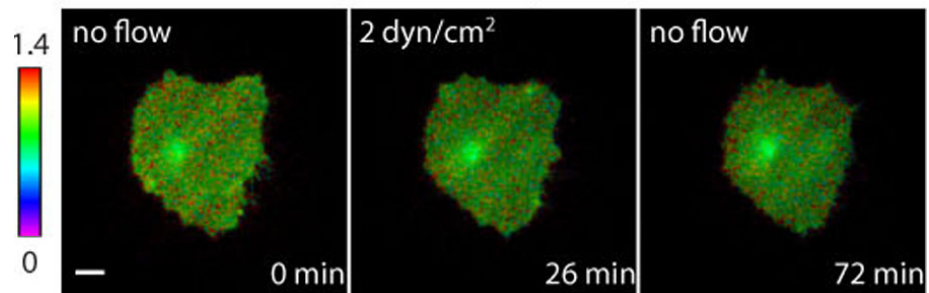
(b)

Fig. 2.3. Shear stress experiment device. (a) Cells were seeded on glass cover slip coated with hydrogel, and applied shear flow inside parallel plate flow chamber (Modified from [35]). (b) Transfected cell plated on μ -slide cell culture chamber (Ibidi), and subjected to shear flow. Arrow denoted flow direction.

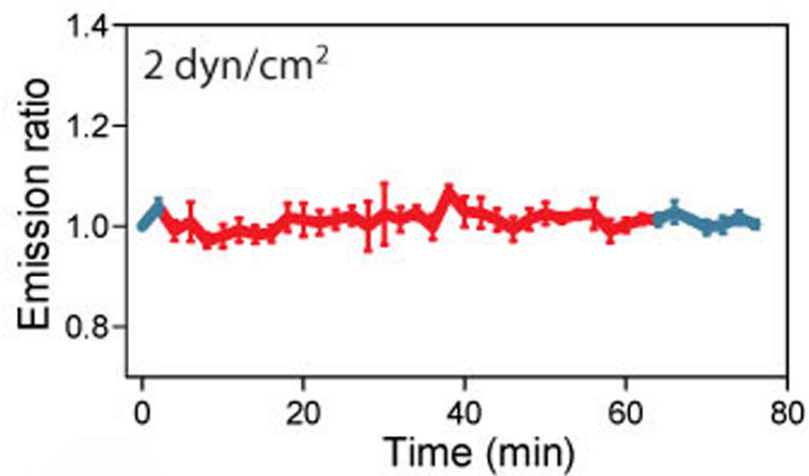
3. RESULTS

3.1 Selective RhoA Activity is Regulated by the Magnitude of Shear Stress

To determine whether the magnitude of the mechanical force can regulate RhoA activities, we transfected a FRET-based, CFP-YFP RhoA biosensor [28] into C28/I2 cells and plated the cells on a type I collagen-coated flow chamber. Spatiotemporal changes of RhoA activities were assessed by monitoring changes on the emission ratio of YFP/CFP of the RhoA biosensor in the cell. The increase of YFP/CFP ratio value represents activation of RhoA activity. During imaging, the cells were subjected to no flow for 2 min, flow-induced shear stress at 2, 5, 10, or 20 dyn/cm² for 1 hr, and lastly no flow for \sim 15 min. RhoA activity was not altered when shear stress of 2 dyn/cm² was applied (Figure 3.1). However, in response to shear stress at 5 dyn/cm², we observed rapid ($<$ 2 min) RhoA inhibition (\sim 15 % FRET decrease; Figure 3.2). When shear stress was removed following the application of 5 dyn/cm², RhoA activity was increased and returned to the basal levels within 10 min (Figure 3.2). In marked contrast to shear stress of 5 dyn/cm², 10 dyn/cm² and 20 dyn/cm² led to slow ($>$ 30 min), but strong RhoA activation (\sim 20% FRET increase; Figure 3.3 and Figure 3.4). These substantially different activity patterns and time courses for RhoA by shear stress suggest that mechanotransduction mechanisms for RhoA activities might be different depending on the magnitude of the applied shear stress.

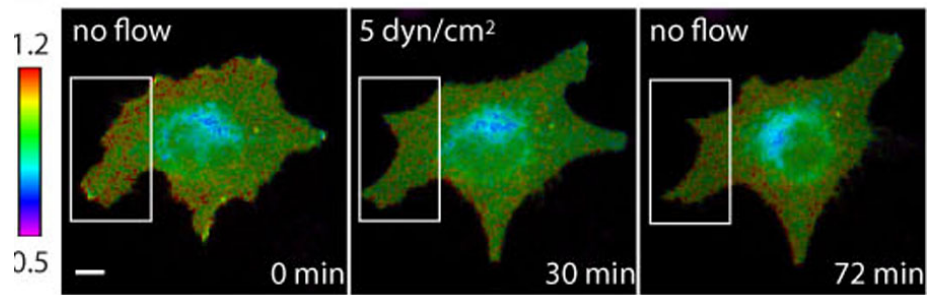


(a)

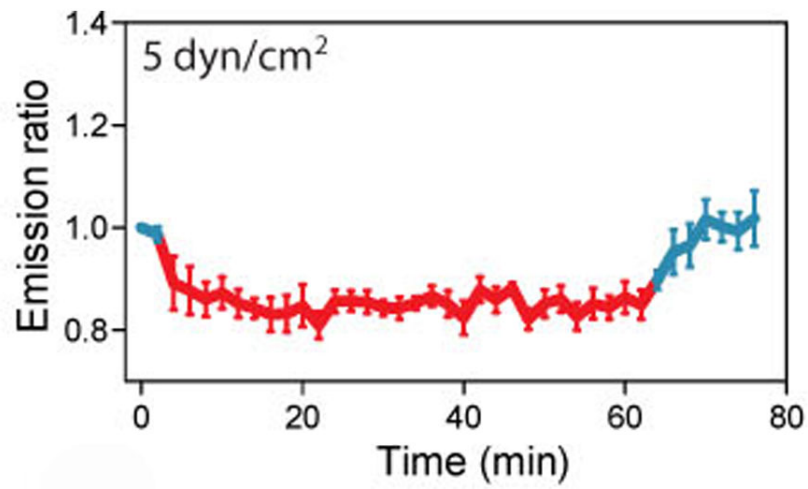


(b)

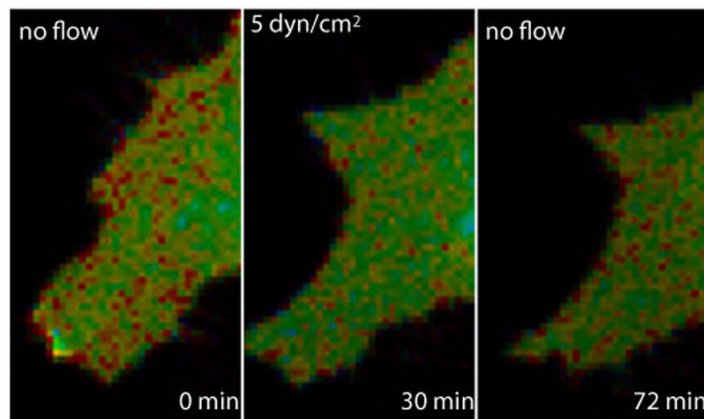
Fig. 3.1. RhoA activity is shear stress-magnitude dependent. RhoA activity was not altered when shear stress of 2 dyn/cm^2 was applied. Shear stress was applied for 1 h. (a) Time course of RhoA activity in response to shear stress. Color bars represent emission ratio of YFP/CFP of the biosensor, an index of RhoA activation. (b) Ratio images of YFP/CFP emission ratio were averaged over the whole cell and were normalized to time point 0 min. Blue color indicates pre- and post-shear stress (no flow), and red color indicates shear stress (2 dyn/cm^2) application. $n = 6$ cells. Scale bars, $10 \mu\text{m}$. Error bars denote s.e.m.



(a)

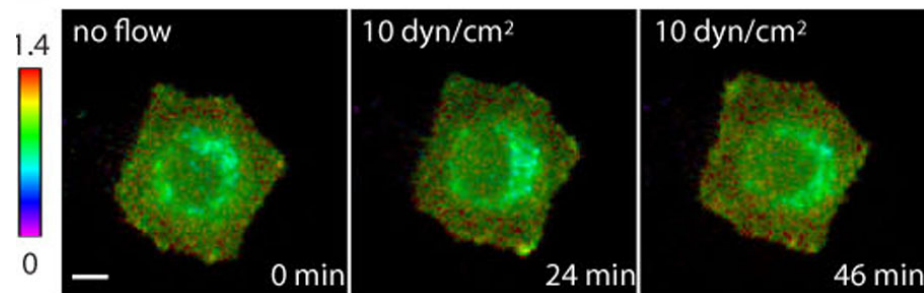


(b)

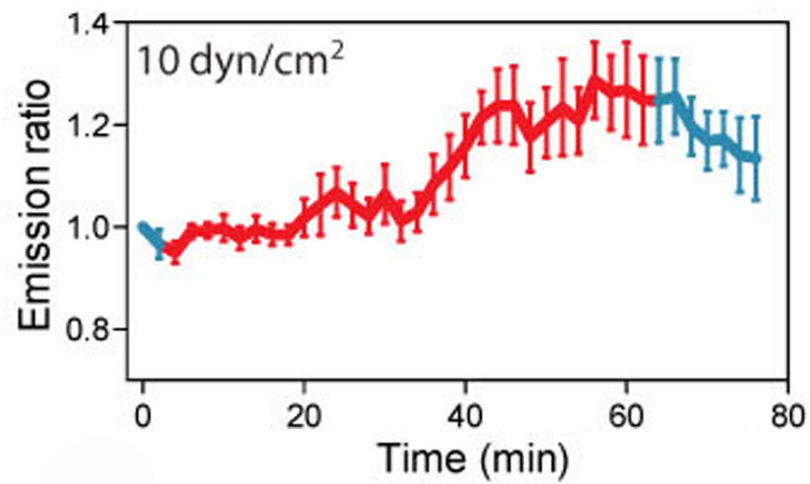


(c)

Fig. 3.2. RhoA activity is shear stress-magnitude dependent. (a,b) In response to shear stress at 5 dyn/cm^2 , RhoA activity is inhibited rapidly. (b) $n = 5$ cells. Scale bars, $10 \mu\text{m}$. Error bars denote s.e.m. The white boxes in 3.2a are cropped and enlarged in 3.2c, for a better visualization.

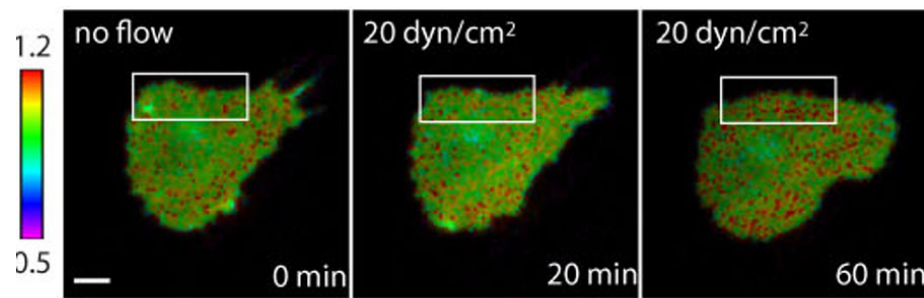


(a)

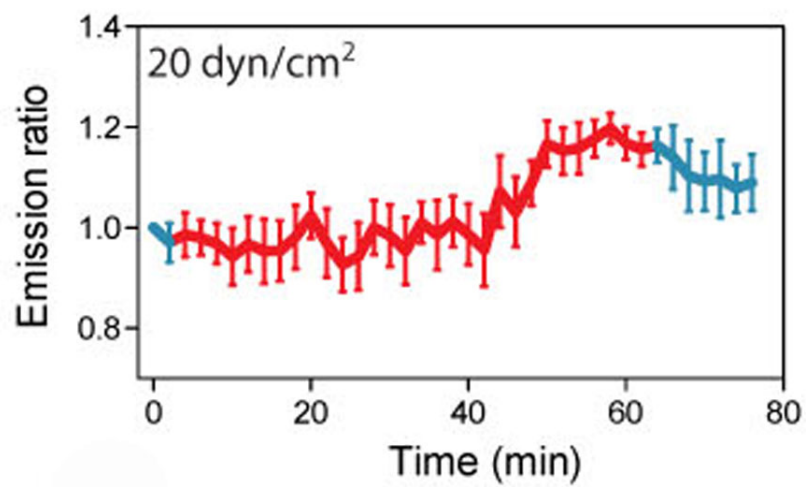


(b)

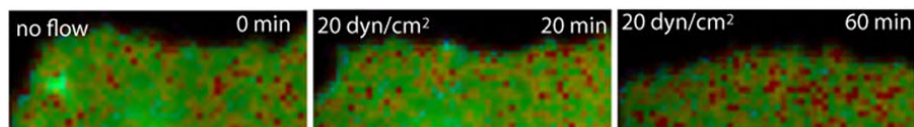
Fig. 3.3. RhoA activity is shear stress-magnitude dependent. (a,b) the application of 10 dyn/cm² shear stress led to slow, but strong RhoA activation. (b) $n = 7$ cells. Scale bars, 10 μm . Error bars denote s.e.m.



(a)

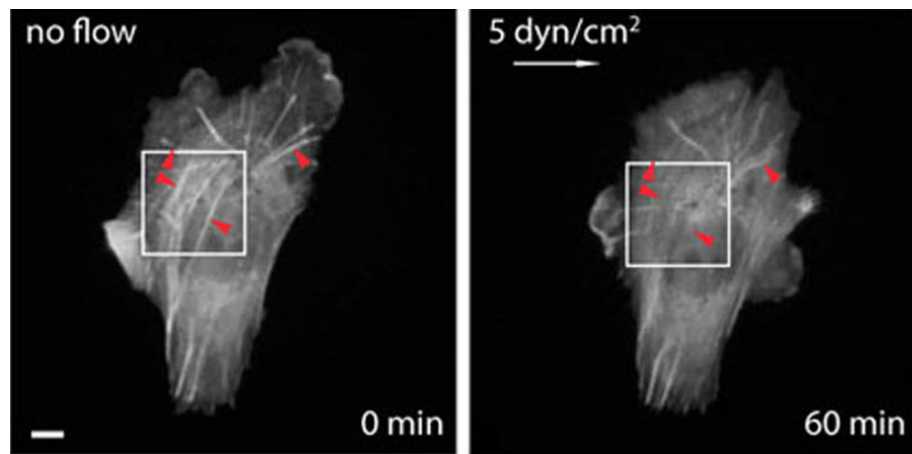


(b)

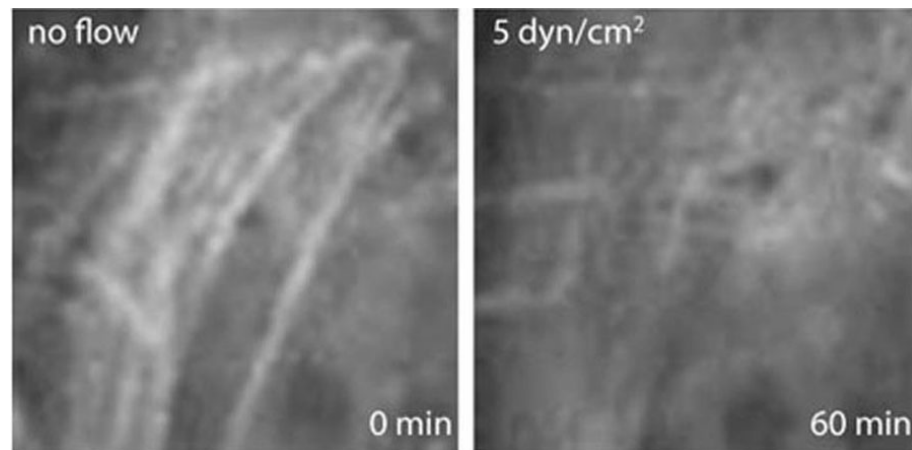


(c)

Fig. 3.4. RhoA activity is shear stress-magnitude dependent. (a,b) 20 dyn/cm^2 led to slow, but strong RhoA activation. (b) $n = 6$ cells. Scale bars, $10 \mu\text{m}$. Error bars denote s.e.m. The white boxes in 3.4a are cropped and enlarged in 3.4c, for a better visualization.

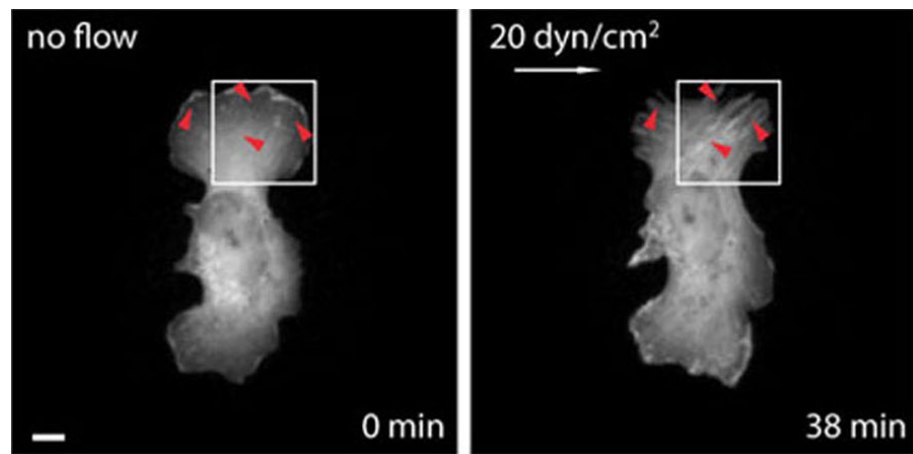


(a)

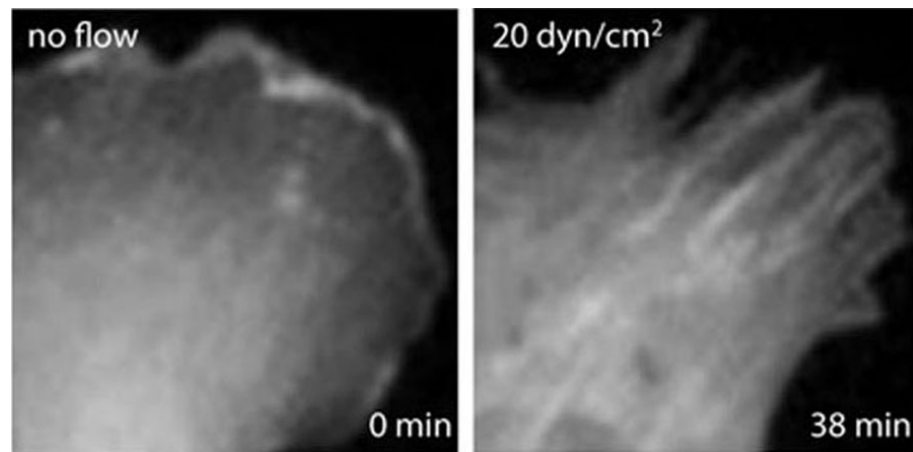


(b)

Fig. 3.5. Shear stress-induced actin cytoskeleton organization is essential for selective RhoA activation. (a) In response to 5 dyn/cm^2 , the cell display a decrease in actin (see arrowheads). Three other different cells showed similar results. (b) The white boxes in 3.5a are cropped and enlarged in 3.5b, for a better visualization. White arrows denote shear flow direction. Scale bars, $10 \mu\text{m}$.



(a)



(b)

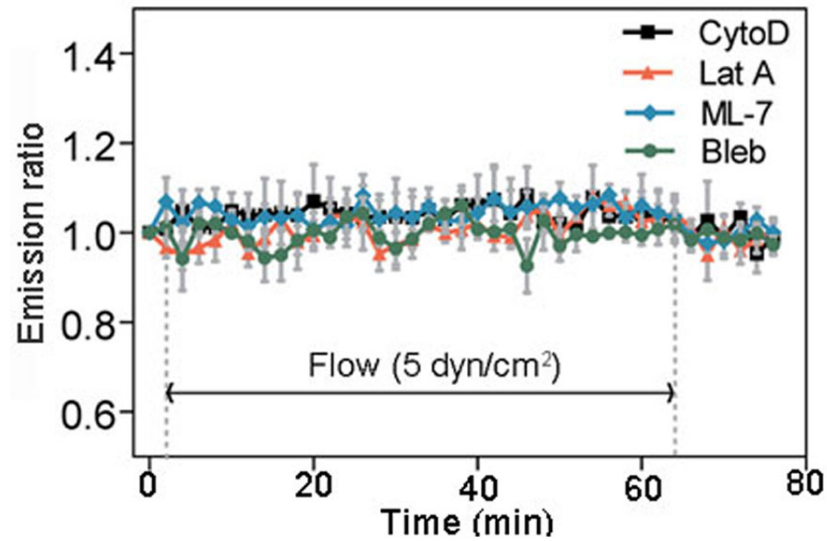
Fig. 3.6. Shear stress-induced actin cytoskeleton organization is essential for selective RhoA activation. (a) In response to 20 dyn/cm², the actin structure increase (see arrowheads). Three other different cells showed similar results. (b) The white boxes in 3.6a are cropped and enlarged in 3.6b, for a better visualization. White arrows denote shear flow direction. Scale bars, 10 μ m.

3.2 Shear Stress-induced RhoA Activity is Correlated with F-actin Remodeling

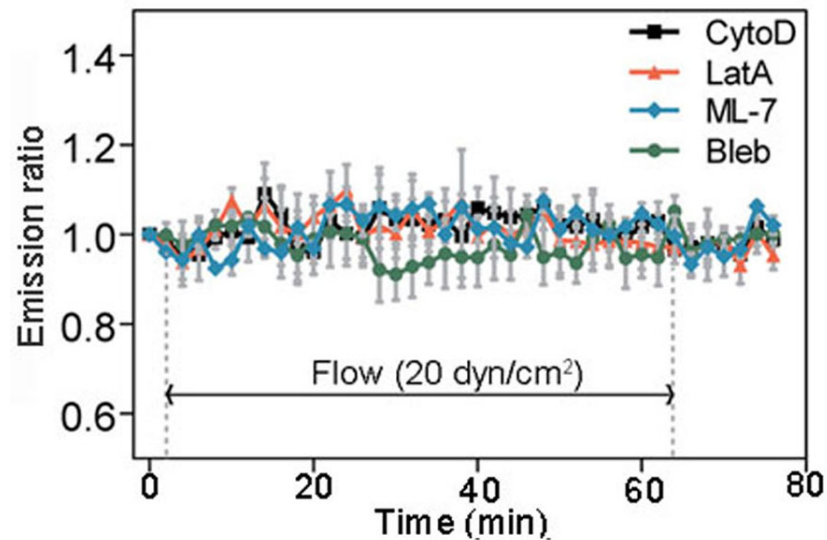
It has been established that shear stress-induced RhoA activity is associated with actin cytoskeleton organization [36]. To determine whether the selective RhoA activities by shear stress, which are shown above, are associated with shear stress-induced changes in actin cytoskeleton organization, we transfected C28 chondrocytes with mCherry-actin and visualized the actin cytoskeletal remodeling while applying shear stress to the cells. In response to shear stress at 5 dyn/cm², actin stress fibers gradually disappeared (Figure 3.5). In contrast, shear stress at 20 dyn/cm² resulted in an increase in actin stress fiber formation (Figure 3.6). These results are correlated with altered RhoA activities by shear stress.

3.3 Actin and Intracellular Tension are Necessary for Shear Stress-induced RhoA Activity

To further explore the potential contribution of actin cytoskeleton in RhoA activity in response to shear stress, we first used the pharmacological inhibitors cytochalasin D (CytoD) or latrunculin A (LatA) to disrupt actin filaments. Cells were pretreated with CytoD or LatA for 15min and subjected to shear stress for 1 hour. Treatment with CytoD or LatA prevented RhoA inhibition and activation by shear stress at 5 and 20 dyn/cm², respectively. We next used ML-7 to inhibit myosin light chain kinase or blebbistatin (Bleb) to inhibit non-muscle myosin II. Pretreating with ML-7 (30 min) or Bleb (20 min) also prevented shear stress-induced RhoA activation and inhibition at corresponding shear stress levels(Figure 3.7). These results demonstrate that the myosin II-dependent, tensed actin cytoskeleton is necessary for selective RhoA regulation by shear stress regardless of the shear stress magnitude.

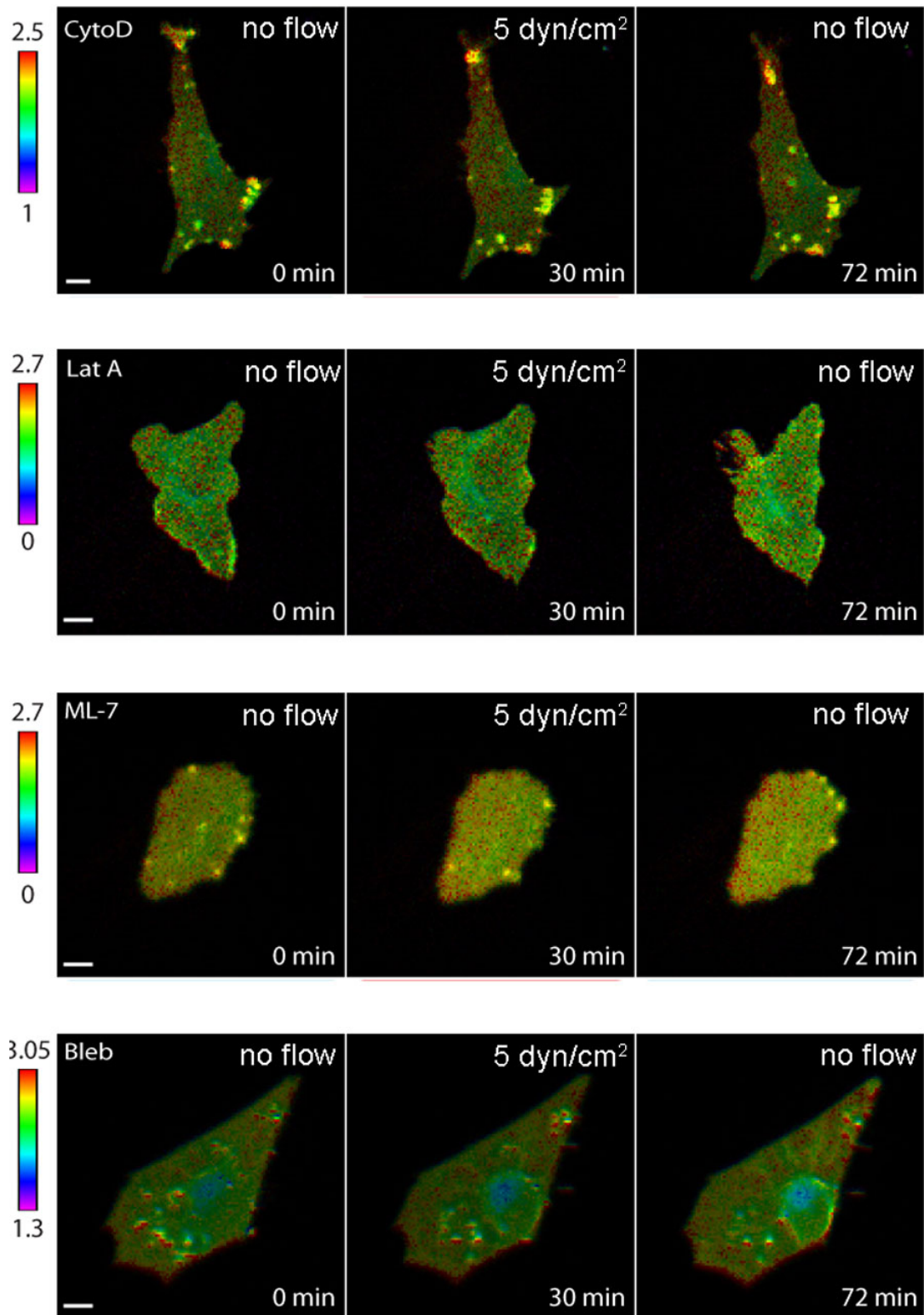


(a)



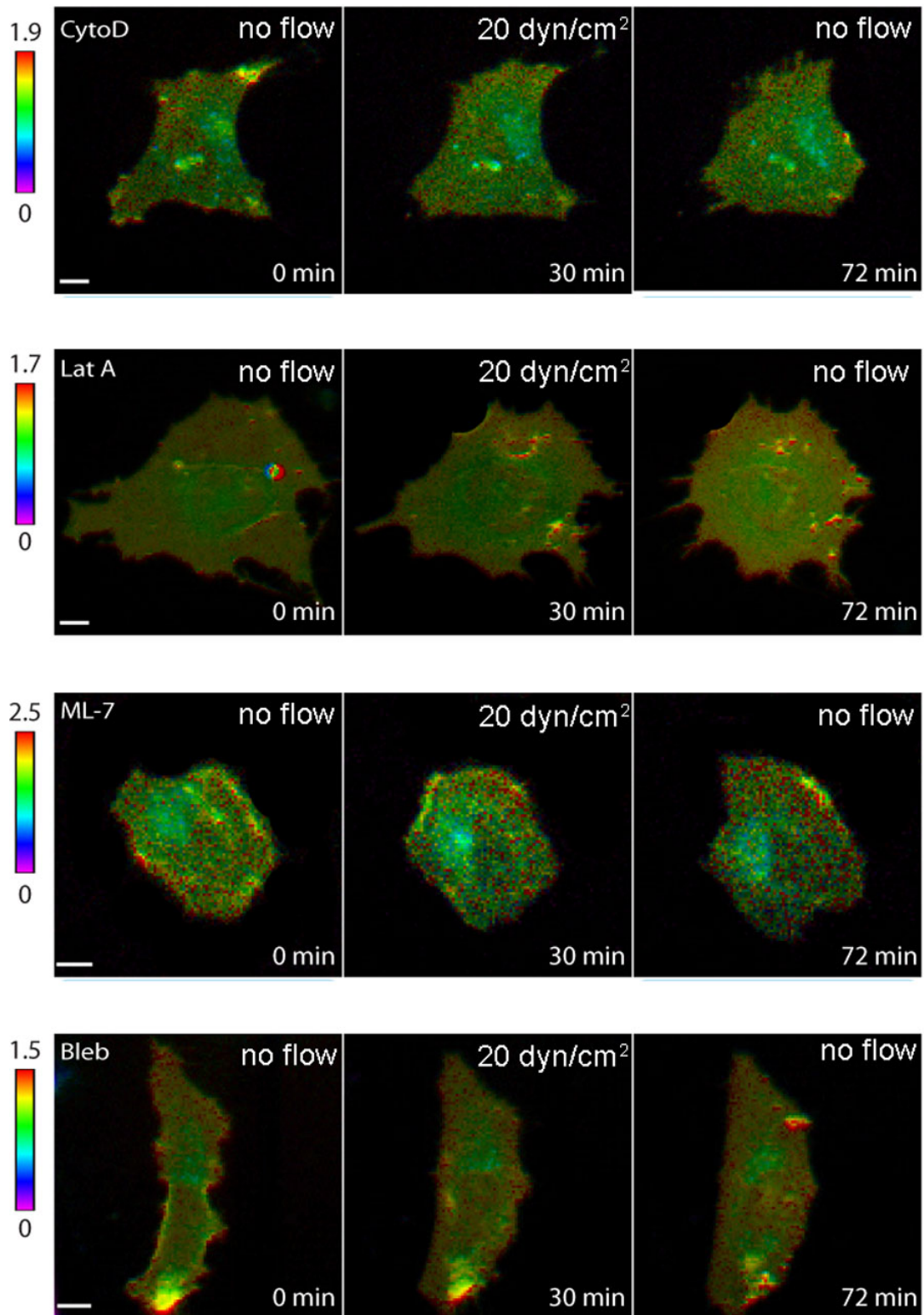
(b)

Fig. 3.7. Shear stress-induced changes in RhoA activity are dependent on actin cytoskeleton and prestress. The cells were transfected with RhoA biosensor and then treated with CytoD ($1 \mu\text{g}/\text{ml}$ for 15 min), LatA ($1 \mu\text{M}$ for 15 min) to disrupt F-actin, ML-7 ($25 \mu\text{M}$ for 30 min) to inhibit myosin light chain kinase, or Bleb ($50 \mu\text{M}$ for 20 min) to inhibit myosin II. (a,b) YFP/CFP ratio images show C28/I2 cells pre-incubated with Cyto D, LatA, ML7, or Bleb prevents RhoA inhibition and activation in response to $5 \text{ dyn}/\text{cm}^2$ and $20 \text{ dyn}/\text{cm}^2$, respectively. (c) $n = 3$ cells for CytoD, $n = 4$ cells for LatA, $n = 4$ cells for ML-7, $n = 2$ cells for Bleb. (d) $n = 4$ cells for CytoD, $n = 3$ cells for LatA, $n = 4$ cells for ML-7, $n = 3$ cells for Bleb. Scale bars, $10 \mu\text{m}$. Error bars denote s.e.m.



(c)

Fig.3.7. Continued



(d)

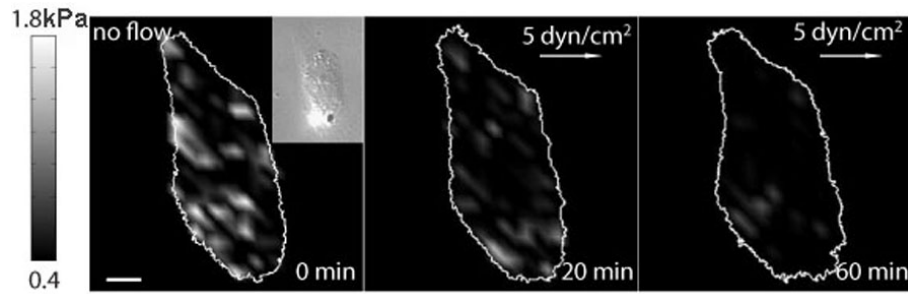
Fig.3.7. Continued

3.4 Shear Stress Regulates Traction Forces

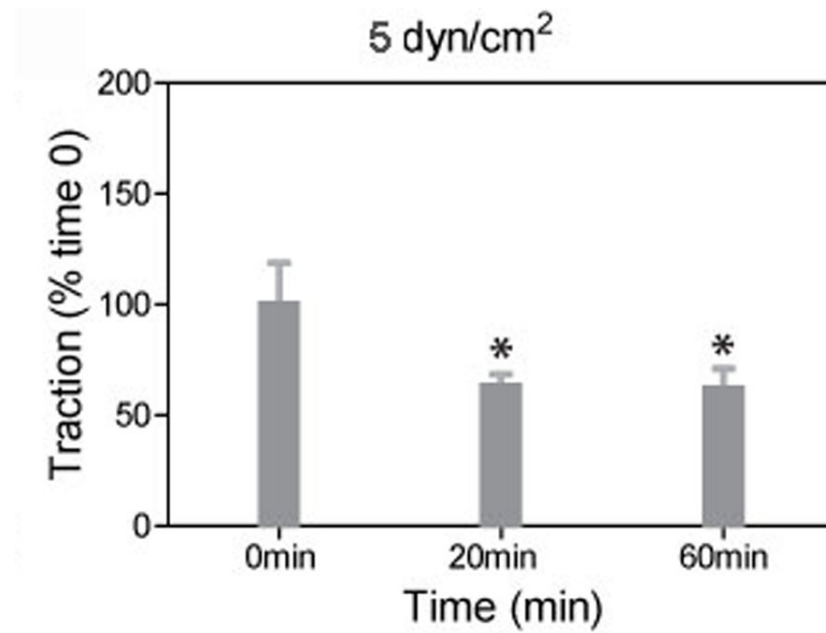
Traction forces are generated within the cell by the actin-myosin contraction [37]. Shear stress of 12 dyn/cm² has been shown to increase both RhoA activity and traction forces of endothelial cells. Because RhoA activation increases traction forces [38], and our results shown that RhoA activities are regulated by shear stress, we postulated that the magnitude of shear stress would regulate traction forces. To test this hypothesis, we quantified changes in tractions in C28 chondrocytes during shear stress application using the traction force microscopy technique [33]. We found that shear stress of 5 dyn/cm² decreased tractions ((~ 30%) within 20 min (Figure 3.8)), and shear stress of 20 dyn/cm² increased tractions substantially ((~ 70%) within 60 min (Figure 3.9)). These results suggest that changes in tractions may be regulated by the magnitude of shear stress. The significant decrease and increase in tractions by 5 dyn/cm² and 20 dyn/cm² in Figure 3.8 and Figure 3.9 was preceded by rapid RhoA modulation by shear stress (see Figure 3.2 and Figure 3.4), suggesting that shear stress magnitude-dependent RhoA activities may be required to regulate shear stress-induced traction dynamics.

3.5 Intermediate Shear Stress Decreases Constitutively Activated RhoA

To further examine the specificity of RhoA in response to shear stress, we co-transfected C28 chondrocytes with a RhoA biosensor and one of either constitutively active (RhoA-V14) or dominant negative (RhoA-N19) mutant of RhoA. To our surprise, shear stress of 5 dyn/cm² still decreased (~15%) RhoA activity of the cell transfected with RhoA-V14 (Figure 3.10). However, shear stress of 20 dyn/cm² failed to further activate RhoA in RhoA-V14-expressing cells (Figure 3.10). The inhibition of RhoA activity by a dominant negative RhoA-N19 or C3 transferase blocked the RhoA regulation by shear stress (Figure 3.11 and Figure 3.12).

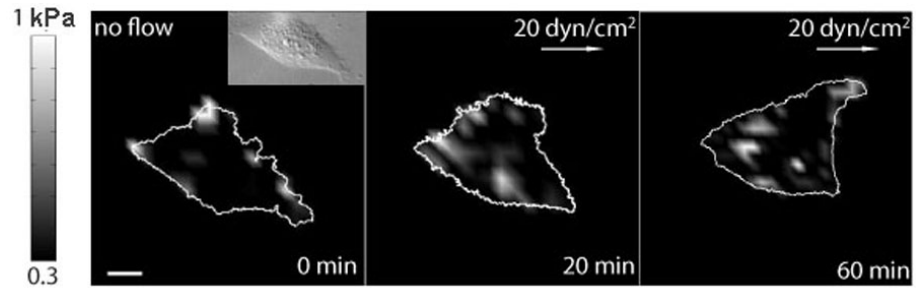


(c)

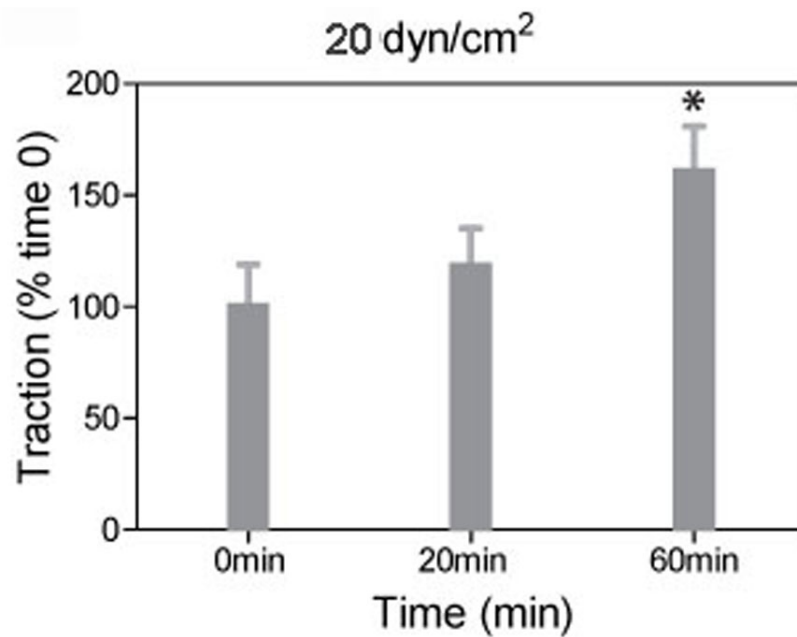


(d)

Fig. 3.8. Dynamic tractions are regulated by stress-magnitude dependent. Dynamic traction maps and time courses of averaged tractions in response to 5 dyn/cm^2 . (a) Color bars represent traction values in pascal (Pa). White arrows indicate shear stress direction. Insets are corresponding DIC images. (b) $n = 5$ cells. Value are normalized by the tractions at 0 min. For the statistical analysis, traction at 20 min and 60 min were compared with traction at 0 min (* $P < 0.05$). Scale bars, $10 \mu\text{m}$. Error bars denote s.e.m.

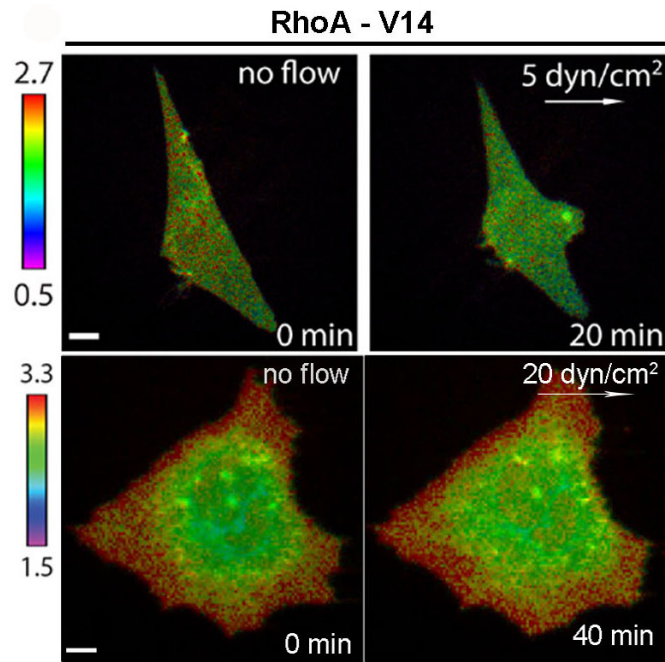


(a)

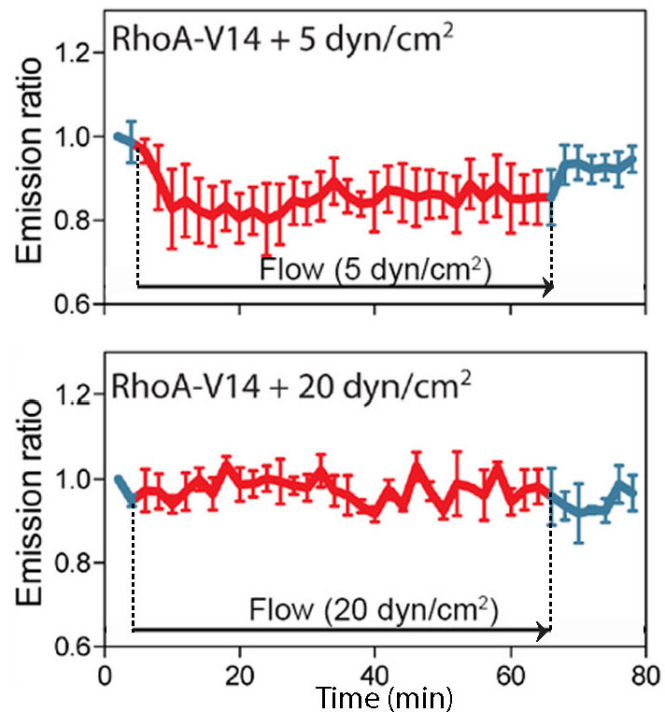


(b)

Fig. 3.9. Dynamic tractions are regulated by stress-magnitude dependent. Dynamic traction maps and time courses of averaged tractions in response to 20 dyn/cm^2 . (a) Color bars represent traction values in pascal (Pa). White arrows indicate shear stress direction. Insets are corresponding DIC images. (b) $n = 5$ cells. Value are normalized by the tractions at 0 min. For the statistical analysis, traction at 60 min were compared with traction at 0 min (* $P < 0.05$). Scale bars, $10 \mu\text{m}$. Error bars denote s.e.m.

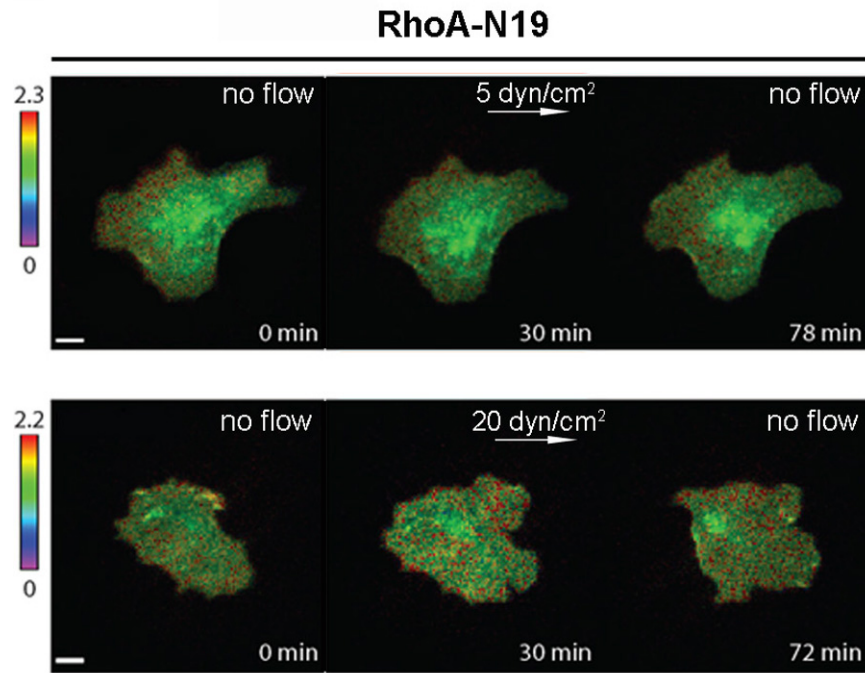


(a)

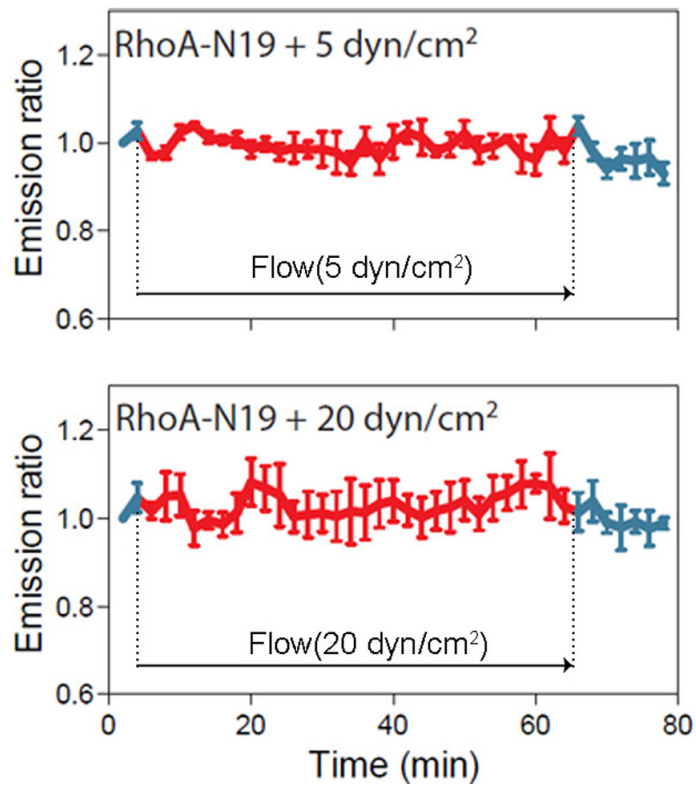


(b)

Fig. 3.10. Shear stress of 5 dyn/cm² downregulate RhoA activity of the cell transfected with a constitutively active RhoA, however, 20 dyn/cm² fail to activate RhoA activity further. (a) RhoA activity decreases in response to 5 dyn/cm² and 20 dyn/cm². White arrows denote shear stress direction. (b) $n = 3$ cells for 5 dyn/cm² and 20 dyn/cm². Scale bars, 10 μ m. Error bars denote s.e.m.

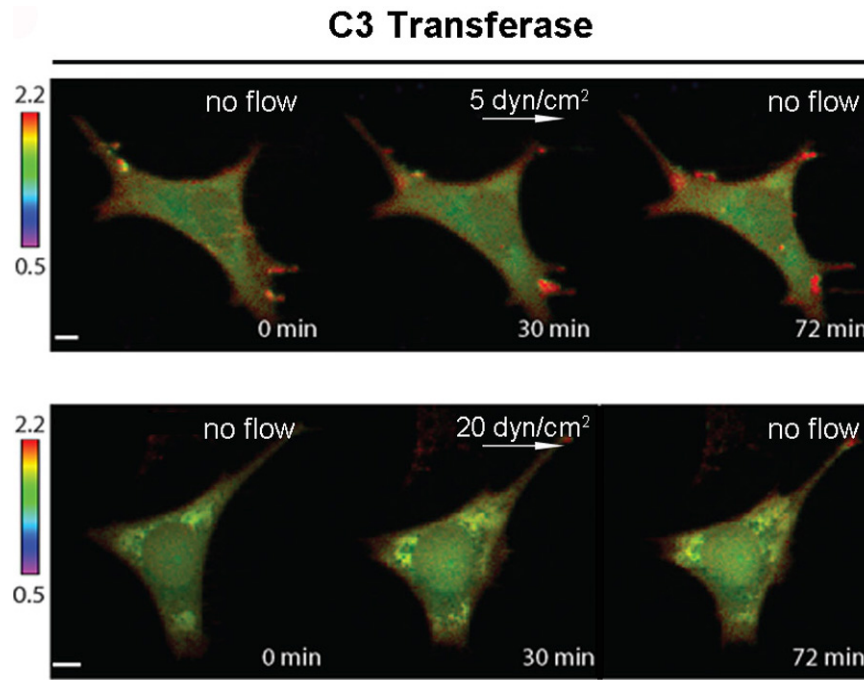


(a)

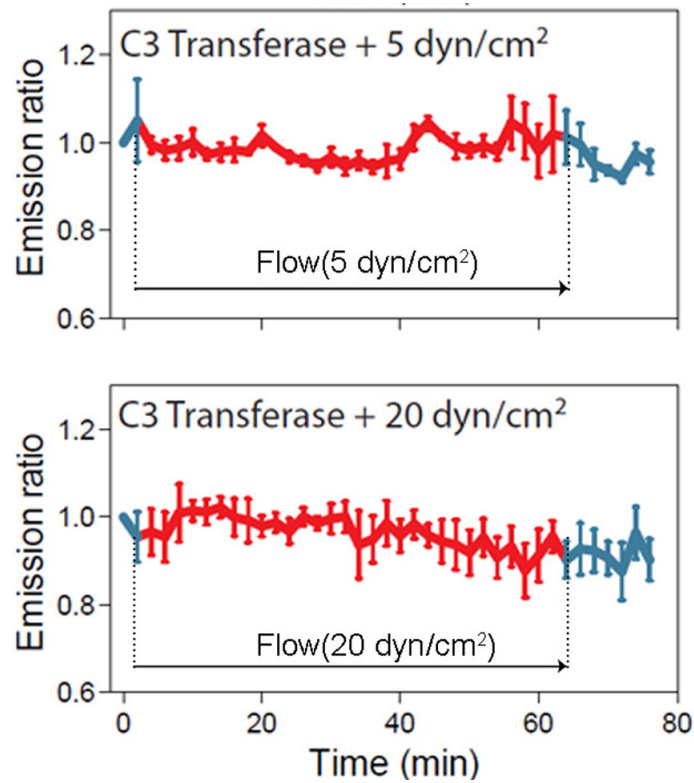


(b)

Fig. 3.11. RhoA-N19 blocked the RhoA regulation by shear stress. (a) The dominant negative N19 RhoA transfection prevents shear stress-induced RhoA activity in both stress conditions. (b) $n=4$ cells for both 5 dyn/cm² and 20 dyn/cm². Scale bars, 10 μm . Error bars denote s.e.m.



(a)



(b)

Fig. 3.12. C3 transferase blocked the RhoA regulation by shear stress. (a) Preincubation of C3 transferase prevents shear-stress-induced RhoA activity in both stress conditions. (b) $n=3$ cells for 5 dyn/cm² and 4 for 20 dyn/cm². Scale bars, 10 μm . Error bars denote s.e.m.

4. DISCUSSION

Using a FRET-based RhoA biosensor, we demonstrated for the first time that RhoA is differentially regulated in C28/I2 chondrocytes depending on the magnitude of shear stress: 5 dyn/cm² reduced RhoA activity, while 10 and 20 dyn/cm² increased it. To date, most studies on mechanotransduction have focused on how mechanical loading can activate intracellular signaling. It has been shown, for instance, that a threshold of mechanical loading or deformation is required to activate the signaling, while the loading lower than the threshold does not directly affect the signaling [14] [39]. However, the molecular mechanism underlying the observed twolevel- switch like regulation of RhoA is apparently different from a simple on-off switch mechanism.

The results herein show that the differential RhoA activity by shear stress is correlated with the alteration in remodeling of actin cytoskeleton. The reduced RhoA activity in response to 5 dyn/cm² corresponds to a decrease in formation of actin stress fibers, while the elevated RhoA activity by 10 or 20 dyn/cm² an increase in their formation. This correlation of RhoA activity to actin organization has been shown in endothelial cells subjected to shear stress of 12 dyn/cm² [16]. although the reported response (a transient decrease followed by an increase) presents a different temporal profile. Chondrocytes are in general rich in cortical actin but poor in cytosolic stress fibers. When they de-differentiate to fibroblast-like cells, they are reported to develop stress fibers [40]. Data in this study suggest that shapes and differentiation states of chondrocytes are regulated differentially by intermediate and high shear stresses [41] [42].

The result in this study also provides the linkage of RhoA activity to force generation. Using the traction force microscopy technique, we observed that dynamics of shear-driven cell contractility are correlated with RhoA activity. Contraction plays an important role in cellular functions including the rates of cell migration as well as

protein synthesis and transport. It is reported that reduced contractility in chondrocytes exhibits higher rates of glycosaminoglycan synthesis [43]. RhoA-induced cell contractility is mediated by Rho kinase (ROCK), which regulates the phosphorylation of myosin light chains and the interaction of actin to myosin II [44]. Thus, shear stress-induced RhoA-ROCK activities could spatially and temporally be correlated with traction force and regulate protein synthesis and transport at a subcellular scale.

A potential mechanism for the observed RhoA regulation in a form of two-level switch might be achieved through interactions with integrins, stress-responsive kinases, and/or other GTPases. Activation of integrins such as $\alpha v \beta 3$ or $\alpha 5 \beta 1$ by shear stress has been shown to transiently downregulate RhoA activity in endothelial cells [16]. Furthermore, shear stress-induced activation of Rac1 [45], or Src [46] is reported to downregulate RhoA activity. Future studies are needed to examine whether the observed two-level regulation of RhoA is mediated through integrins, FAK, Rac1 or Src. We have shown that intermediate shear stress at 5 dyn/cm² downregulates RhoA activity in chondrocytes, which express constitutively active RhoA. It is thus possible that the Rho GDP dissociation inhibitor (Rho-GDI), one of the known Rho GTPase regulators, is involved in the observed regulation of RhoA activity, since Rho-GDI is known to be responsive to shear stress and cyclic stretching [47] [48].

In summary, we demonstrate that shear stress regulates RhoA activity in a stress-magnitudedependent manner, and that the differential activity of RhoA by shear stress is associated with the dynamical alterations in cytoskeletal remodeling and traction force. The results presented here suggest that load-driven changes in RhoA activity affect cytoskeletal organization and dynamic force generation in chondrocytes. Future studies will address how RhoA interacts with other Rho family GTPases such as Rac1 and Cdc42 under mechanical loading and how the load-induced GTPases are involved in metalloproteinase activities in chondrocytes.

LIST OF REFERENCES

LIST OF REFERENCES

- [1] D. E. Discher, P. Janmey, and Y. L. Wang, "Tissue cells feel and respond to the stiffness of their substrate," *Science*, vol. 310, no. 5751, pp. 1139–1143, 2005.
- [2] G. Giannone and M. P. Sheetz, "Substrate rigidity and force define form through tyrosine phosphatase and kinase pathways," *Trends in cell biology*, vol. 16, no. 4, pp. 213–223, 2006.
- [3] P. A. Janmey and C. A. McCulloch, "Cell mechanics: integrating cell response to mechanical stimuli," *Annual Review of Biomedical Engineering*, vol. 9, no. 9, pp. 1–34, 2007.
- [4] "What is articular cartilage." <http://www.thaimedicalnews.com/about-knee-problems-damaged-articular-cartilage-treatments/2008/05/08/>. Last accessed May 2012.
- [5] H. Yokota, M. B. Goldring, and H. B. Sun, "Cited2-mediated regulation of mmp-1 and mmp-13 in human chondrocytes under flow shear," *The journal of biological chemistry*, vol. 278, no. 47, pp. 47275–47280, 2003.
- [6] J. K. Suh, G. H. Baek, A. Aroen, C. M. Malin, C. Niyibizi, C. H. Evans, and A. Westerhausen-Larson, "Intermittent sub-ambient interstitial hydrostatic pressure as a potential mechanical stimulator for chondrocyte metabolism," *Osteoarthritis Cartilage*, vol. 7, no. 1, pp. 71–80, 1999.
- [7] D. E. Ingber, "Mechanobiology and diseases of mechanotransduction," *Annals of Medicine*, vol. 35, no. 8, pp. 564–577, 2003.
- [8] D. E. Jaalouk and J. Lammerding, "Mechanotransduction gone awry," *Molecular cell biology*, vol. 10, no. 1, pp. 63–73, 2009.
- [9] H. Yokota, D. J. Leong, and H. B. Sun, "Mechanical loading: bone remodeling and cartilage maintenance," *Current Osteoporosis Reports*, vol. 9, no. 4, pp. 237–242, 2011.
- [10] V. Vogel and M. Sheetz, "Local force and geometry sensing regulate cell functions," *Nature Reviews Molecular Cell Biology*, vol. 7, no. 7, pp. 265–275, 2006.
- [11] C. P. Johnson, H. Y. Tang, C. Carag, D. W. Speicher, and D. E. Discher, "Forced unfolding of proteins within cells," *Science*, vol. 317, no. 5838, pp. 663–666, 2007.
- [12] Y. Wang, E. L. Botvinick, Y. Zhao, M. W. Berns, S. Usami, R. Y. Tsien, and S. Chien, "Visualizing the mechanical activation of src," *Nature*, vol. 434, no. 7036, pp. 1040–1045, 2005.

- [13] Y. Sawada, M. Tamada, B. J. Dubin-Thaler, O. Cherniavskaya, R. Sakai, S. Tanaka, and M. P. Sheetz, "Force sensing by mechanical extension of the src family kinase substrate p130cas," *Cell*, vol. 127, no. 5, pp. 1015–1026, 2006.
- [14] S. Na, O. Collin, F. Chowdhury, B. Tay, M. Ouyang, Y. Wang, and N. Wang, "Rapid signal transduction in living cells is a unique feature of mechanotransduction," *Proceedings of the National Academy of Sciences*, vol. 105, no. 5, pp. 6626–6631, 2008.
- [15] E. Tzima, M. A. del Pozo, S. J. Shattil, S. Chien, and M. A. Schwartz, "Activation of integrins in endothelial cells by fluid shear stress mediates rho-dependent cytoskeletal alignment," *The EMBO journal*, vol. 20, no. 17, pp. 4639–4647, 2001.
- [16] Y. T. Shiu, S. Li, W. A. Marganski, S. Usami, M. A. Schwartz, Y. L. Wang, M. Dembo, and S. Chien, "Rho mediates the shear-enhancement of endothelial cell migration and traction force generation," *Biophysical Journal*, vol. 86, no. 4, pp. 2558–2565, 2004.
- [17] B. Wojciak-Stothard and A. J. Ridley, "Shear stress-induced endothelial cell polarization is mediated by rho and rac but not cdc42 or pi 3-kinase," *The Journal of Cell Biology*, vol. 161, no. 2, pp. 429–439, 2003.
- [18] A. J. Putnam, J. J. Cunningham, B. B. Pillemer, and D. J. Mooney, "External mechanical strain regulates membrane targeting of rho gtpases by controlling microtubule assembly," *American Journal of Physiology - Cell Physiology*, vol. 284, no. 3, pp. c627–639, 2003.
- [19] P. G. Smith, C. Roy, Y. N. Zhang, and S. Chaudhuri, "Mechanical stress increases rhoa activation in airway smooth muscle cells," *American journal of respiratory cell and molecular biology*, vol. 28, no. 4, pp. 436–442, 2003.
- [20] S. Kawamura, S. Miyamoto, and J. H. Brown, "Initiation and transduction of stretch-induced rhoa and rac1 activation through caveolae: cytoskeletal regulation of erk translocation," *The Journal of Biological Chemistry*, vol. 276, no. 33, pp. 24843–24854, 2003.
- [21] D. R. Haudenschild, B. Nguyen, J. Chen, D. D. D. Lima, and M. K. Lotz, "Rho kinase-dependent ccl20 induced by dynamic compression of human chondrocytes," *Arthritis and rheumatism*, vol. 58, no. 9, pp. 2735–2742, 2008.
- [22] D. R. Haudenschild, J. Chen, N. Pang, M. K. Lotz, and D. D. D. Lima, "Rho kinase-dependent activation of sox9 in chondrocytes," *Arthritis and rheumatism*, vol. 62, no. 1, pp. 191–200, 2010.
- [23] C. Guilluy, V. Swaminathan, R. Garcia-Mata, E. T. O'Brien, R. Superfine, and K. Burridge, "The rho gefs larg and gef-h1 regulate the mechanical response to force on integrins," *Nature cell biology*, vol. 13, no. 6, pp. 722–727, 2011.
- [24] M. F. Olson, "Contraction reaction: mechanical regulation of rho gtpase," *Trends in cell biology*, vol. 14, no. 3, pp. 111–114, 2004.
- [25] A. B. Jaffe and A. Hall, "Rho gtpases: biochemistry and biology," *Annual Review of Cell and Developmental Biology*, vol. 21, no. 21, pp. 247–269, 2005.

- [26] A. Ridley, “Rho gtpases: Integrating integrin signaling,” *The Journal of Cell Biology*, vol. 150, no. 4, pp. F107–109, 2000.
- [27] S. Etienne-Manneville and A. Hall, “Rho gtpases in cell biology,” *Nature*, vol. 420, no. 6916, pp. 629–635, 2002.
- [28] H. Yoshizaki, Y. Ohba, K. Kurokawa, R. E. Itoh, T. Nakamura, N. Mochizuki, K. Nagashima, and M. Matsuda, “Activity of rho-family gtpases during cell division as visualized with fret-based probes,” *Journal of Cell Biology*, vol. 162, no. 2, pp. 233–232, 2003.
- [29] S. Li, B. P. Chen, N. Azuma, Y. L. Hu, S. Z. Wu, B. E. Sumpio, J. Y. Shyy, and S. Chien, “Distinct roles for the small gtpases cdc42 and rhoa in endothelial responses to shear stress,” *Journal of Clinical Investigation*, vol. 103, no. 8, pp. 1141–1150, 1999.
- [30] M. B. Goldring, J. R. Birkhead, and J. F. Apperley, “Interleukin-1 beta-modulated gene expression in immortalized human chondrocytes,” *The Journal of Clinical Investigation*, vol. 94, no. 6, pp. 2307–3316, 1994.
- [31] R. J. Pelham and Y. Wang, “Cell locomotion and focal adhesions are regulated by substrate flexibility,” *Proceedings of the National Academy of Sciences of the United States of America*, vol. 94, no. 25, pp. 13661–13665, 1997.
- [32] S. Park, K. D. Costa, G. A. Ateshian, and K. S. Hong, “Mechanical properties of bovine articular cartilage under microscale indentation loading from atomic force microscopy,” *Proceedings of the Institution of Mechanical Engineers. Part H*, vol. 223, no. 3, pp. 339–347, 2009.
- [33] J. P. Bulter, I. M. Tolic-Norrelykke, B. Fabry, and J. J. Fredberg, “Traction fields, moments, and strain energy that cells exert on their surroundings,” *American Journal of Physiology - Cell Physiology*, vol. 282, no. 3, pp. 595–605, 2002.
- [34] P. Roy, Z. Rajfur, P. Pomorski, and K. Jacobson, “Microscope-based techniques to study cell adhesion and migration,” *Nature Cell Biology*, vol. 4, no. 4, pp. E91–E96, 2002.
- [35] K. A. Addae-Mensah and J. P. Wikswo, “Measurement techniques for cellular biomechanics in vitro,” *Experimental Biology and Medicine*, vol. 233, no. 7, pp. 792–809, 2008.
- [36] E. Tzima, M. A. del Pozo, S. J. Shattil, S. Chien, and M. A. Schwartz, “Activation of integrins in endothelial cells by fluid shear stress mediates rho-dependent cytoskeletal alignment,” *The EMBO Journal*, vol. 20, no. 17, pp. 4639–4647, 2001.
- [37] K. A. Beningo and Y. L. Wang, “Flexible substrate for the detection of cellular traction forces,” *Trends in Cell Biology*, vol. 12, no. 2, pp. 79–84, 2002.
- [38] M. Chrzanowska-Wodnicka and K. Burridge, “Rho-stimulated contractility drives the formation of stress fibers and focal adhesions,” *The Journal of Cell Biology*, vol. 133, no. 6, pp. 1403–1415, 1996.
- [39] Y. C. Poh, S. Na, F. Chowdhury, M. Ouyang, Y. Wang, and N. Wang, “Rapid activation of rac gtpase in living cells by force is independent of src,” *PLoS ONE*, vol. 4, no. 11, p. e7886, 2009.

- [40] C. R. Lee, A. J. Grodzinsky, and M. Spector, "Modulation of the contractile and biosynthetic activity of chondrocytes seeded in collagen-glycosaminoglycan matrices," *Tissue Engineering*, vol. 9, no. 1, pp. 27–36, 2003.
- [41] E. Langelier, R. Suetterlin, C. D. Hoemann, U. Aebi, and M. D. Buschmann, "The chondrocyte cytoskeleton in mature articular cartilage: structure and distribution of actin, tubulin, and vimentin filaments," *Journal of Histochemistry and Cytochemistry*, vol. 48, no. 10, pp. 1307–1320, 2000.
- [42] A. Woods, G. Wang, and F. Beier, "Rhoa/rock signaling regulates sox9 expression and actin organization during chondrogenesis," *The Journal of Biological Chemistry*, vol. 280, no. 12, pp. 11626–11634, 2005.
- [43] M. Amano, K. Chihara, K. Kimura, Y. Fukata, N. Nakamura, Y. Matsuura, and K. Kaibuchi, "Formation of actin stress fibers and focal adhesions enhanced by rho-kinase," *Science*, vol. 275, no. 5304, pp. 1308–1311, 1997.
- [44] F. Beier and R. F. Loeser, "Biology and pathology of rho gtpase, pi-3 kinase-akt, and map kinase signaling pathways in chondrocytes," *Journal of Cellular Biochemistry*, vol. 110, no. 3, pp. 573–580, 2010.
- [45] W. T. Arthur, L. A. Petch, and K. Burridge, "Integrin engagement suppresses rhoa activity via a c-src-dependent mechanism," *Current Biology*, vol. 10, no. 12, pp. 719–722, 2000.
- [46] D. R. Haudenschild, D. D. D’Lima, and M. K. Lotz, "Dynamic compression of chondrocytes induces a rho kinase-dependent reorganization of the actin cytoskeleton," *Biorheology*, vol. 45, no. 3-4, pp. 219–228, 2008.
- [47] Y. X. Q, M. J. Qu, D. K. Long, B. Liu, Q. P. Yao, S. Chien, and Z. L. Jiang, "Rho-gdp dissociation inhibitor alpha downregulated by low shear stress promotes vascular smooth muscle cell migration and apoptosis: a proteomic analysis," *Cardiovascular research*, vol. 80, no. 1, pp. 114–122, 2008.
- [48] A. Kumar, R. Murphy, P. Robinson, L. Wei, and A. M. Boriek, "Cyclic mechanical strain inhibits skeletal myogenesis through activation of focal adhesion kinase, rac-1 gtpase, and nf-kappab transcription factor," *The FASEB Journal*, vol. 18, no. 13, pp. 1524–1535, 2004.